Dependence of Nonlinear Optical Response of Anatase TiO_2 on Shape and Excitation Intensity *

Lu-Hua Guo(郭路华), Ying-Wei Wang(王迎威), Yong-Qiang Jiang(蒋永强), Si Xiao(肖思)**, Jun He(何军)**

Hunan Key Laboratory of Super Microstructure and Ultrafast Process, School of Physics and Electronics, Central South University, Changsha 410083

(Received 14 March 2017)

Nonlinear optical (NLO) properties of anatase TiO_2 with nanostructures of nanoparticle (NP), nanowire (NW) and annealed nanowire (NWA) are studied by open-aperture and closed-aperture Z-scan techniques with a femtosecond pulsed laser at wavelengths of 532 nm and 780 nm simultaneously. At 532 nm, when increasing excitation intensity, NLO absorption of TiO_2 NPs transforms from saturable absorption to reverse-saturable absorption. However, NWs and NWAs exhibit the opposite change. At 780 nm, all samples show reverse-saturable absorption, but have different sensitivities to excitation intensity. Due to the larger surface-to-volume ratio of NPs and less defects of NWAs by annealing, nonlinear optical absorption coefficients follow the order NPs≥NWs≥NWAs. The results also show that these shape and annealing effects are dominant at low excitation intensity, but do not exhibit at the high excitation intensity. The NLO refractive index of NPs shows a positive linear relationship with the excitation intensity, whereas NW and NWAs exhibit a negative linear relationship. The results could provide some foundational guidance to applications of anatase TiO_2 in optoelectronic devices or other aspects.

PACS: 78.67.−n, 78.67.Bf, 78.67.Uh, 42.65.−k DOI: 10.1088/0256-307X/34/7/077803

Since Fujishima and Honda[1] discovered the phenomenon of photocatalytic water splitting with TiO_2 as an electrode in 1972, TiO_2 has been extensively investigated. TiO_2 has many characteristics such as being inexpensive, non-toxic, having good mechanical durability, superior biological, chemical and physical stability, excellent photostability, and a high direct band gap of circa 3.2 eV.[2,3] These properties make it play an irreplaceable role in applications of paint,[3] photocatalysis,[4] wastewater treatment,[5] biosensors,[6,7] gas sensors,[8] ion detection,[9] solar cells[10−12] and printed elctronics.[10,11] In recent years, the nanotechnologies have obtained great improvement in synthesis of nanomaterials with well-controlled size, shape and surface properties. The synthesized TiO_2 particle size can range from circa 5 nm to several millimeters.[13,14] Its crystalline phase can be anatase, rutile or brookite[2,14] and the shapes of anatase are also diverse, i.e., nanoparticle, nanosheet, nanorod, nanowire, nanotube and nanoflower.[15] All of these technologies promote the developments of experimental and theoretical researches about TiO_2.

Materials with large nonlinear optical response are useful in applications of optical communications, information storage, optoelectronic devices and laser protective devices. To seek materials with better optical performance, researchers have studied many kinds of materials, including bulk semiconductors,[16,17] quantum dots[18] and various novel 2D materials.[19−21] As we all know, TiO_2 is a common semiconductor. Before the femtosecond pulsed laser was widely used, the nonlinear optical response of TiO_2 has also been investigated in previous works. Elim *et al.* observed large optical nonlinearities in PMMA-TiO_2 nanocomposites using the Z-scan technique caused by two-photon resonant excitation, $\beta = 1.4 \times 10^{-8}$ m/W and $n_2 = 2.5 \times 10^{-15}$ m^2/W.[22] Gayvoronsky *et al.* also obtained a giant nonlinear optical (NLO) refraction of anatase TiO_2 nanoporous layers with picosecond laser exciting in the four-wave mixing technique. The extracted third-order NLO susceptibility is approximately $\chi^{(3)} = 2 \times 10^{-5}$ esu, which is even larger and explained as the effect of the surface defects on anatase NPs.[23] However, Portuondo-Campa *et al.* obtained a small NLO refraction index in nanoporous anatase nanoparticle film of 10^{-19} m^2/W^{-1} using the optical Kerr effect technique.[3] Divya *et al.* found that anatase TiO_2 shows a better limiting capability than the amorphous and rutile phase of TiO_2.[24] Anatase TiO_2 with a nanoflower structure shows higher nonlinear absorption and nonlinear refraction than that of other structures. This is attributed to its high surface-to-volume ratio and intertwined petal-like structure.[15] Elim *et al.* investigated the pure third-order nonlinear processes of PMMA-TiO_2 films (T60), both the nonlinear absorption coefficient and nonlinear refractive index are independent of the light intensity with 780 nm, 250 fs laser exciting.[22] However, Zhang *et al.* observed a change of nonlinear absorption of anatase TiO_2 nanowires from reverse-saturable absorption to saturable absorption with excitation energy increased at 532 nm and 25 ps.[25]

From the above results, it is known that NLO properties of TiO_2 have obtained a great deal of attention and many factors can affect its optical nonlinearities, including crystalline, morphology and excitation intensity. However, more studies about the NLO response of anatase with respect to the shape and incident intensity are needed. To systematically investigate the dependence of the optical nonlinearities of anatase TiO_2 on excitation intensity, we study

*Supported by the National Natural Science Foundation of China under Grant Nos 11404410 and 11504105.
**Corresponding author. Email: sixiao@csu.edu.cn; junhe@csu.edu.cn
© 2017 Chinese Physical Society and IOP Publishing Ltd

the nonlinear optical response of anatase NPs, NWs and NWAs using the Z-scan technique with different excitation intensities at both 532 nm and 780 nm simultaneously.

Powders of anatase TiO_2 NPs, NWs and NWAs were provided by Zhaoyang Fan (Texas Tech University). The original material, i.e., TiO_2 Degussa P25 NPs powders, was produced by the EVONIK industry. Using TiO_2 Degussa P25 NPs, single crystalline TiO_2 NWs were synthesized with the hydrothermal method, and the TiO_2 NWs were baked at 70℃ for 6 h, then TiO_2 NWAs were obtained.[26] The size and shape of the samples were characterized using a transmission electron microscope (TEM) (Tecnai G2 F20 S-TWIX). A double-beam ultraviolet (UV) visible spectrophotometer (T9 series) was used to measure linear optical properties of the samples which were dispersed in deionized water. The nonlinear optical properties of the samples were measured with open-aperture and closed-aperture Z-scan techniques. The schematic diagram of the experimental setup can be available in the literature.[21,27] The laser source in the Z-scan experiment was 532 nm and 780 nm with repetition rate of 2 kHz, 35 fs. The laser was focused by a thin convex lens ($f = 150$ mm). A laser probe detector (Laserprbe Rm-6600) was used to collect the transmittance intensity through the samples as a function of the sample position z with and without an aperture in the far field before the detector. The samples were dispersed in deionized water and filled in quartz cuvettes with the thickness of $L = 1$ mm. The beam waist radius at the focus of the lens at 532 nm and 780 nm was 29.3 μm and 37.2 μm, respectively. According to the formula of the Rayleigh length ($Z_0 = \pi\omega_0^2/\lambda$), values of Z_0 are 5.07 mm and 5.57 mm, respectively, and $Z_0 > L$. It is demonstrated that the quartz cuvette can be regarded as a thin sample in Z-scan experiments, which satisfies the precondition of Z-scan techniques.[27]

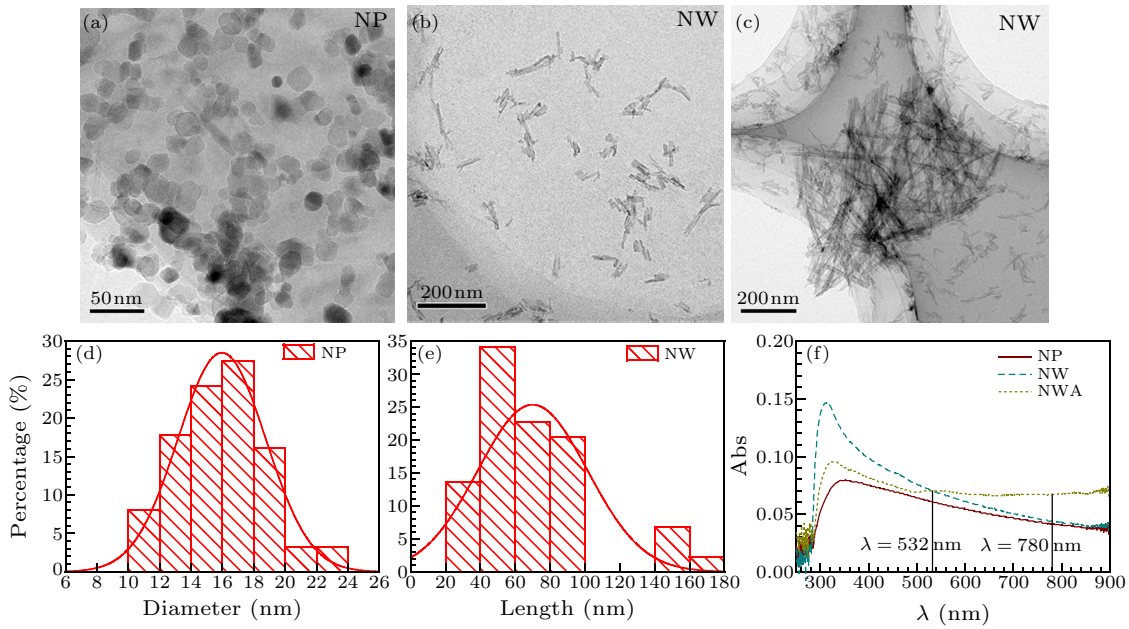

Fig. 1. TEM images of the anatase TiO_2 NPs (a) and NWs [(b), (c)]. Statistical analysis of (d) the diameters of NPs and (e) lengths of NWs measured from TEM images (a) and (b). (f) UV-vis spectra of TiO_2 NPs, NWs and NWAs.

Figures 1(a)–1(c) are the TEM images of anatase TiO_2 NPs and NWs. It can be seen that sizes of the obtained TiO_2 NPs are relatively uniform and TiO_2 NWs have an obvious wire-like morphology. The degree of accumulation in suspensions varies with respect to shape and size. Figures 1(b) and (c) are shorter NWs and longer NWs, respectively. It can be seen that NWs with higher length show a higher degree of accumulation than NPs and the shorter NWs. Figures 1(d) and 1(e) are the statistical analysis of diameters of NPs and lengths of the shorter dispersed NWs from the TEM images shown in Figs. 1(a) and 1(b). The diameters of NPs and of NWs are approximately 16 nm and 6 nm, respectively. The average length of the shorter dispersed NWs is 70 nm, and the length of the aggregative NWs can be 400 nm. The TEM images of TiO_2 NWAs are similar to those of NWs. TiO_2 NWAs also have a wire-like morphology and their diameters are about 7 nm. Lengths of TiO_2 NWs are also nonuniform and vary from ∼43 nm to 220 nm. Figure 1(f) depicts the UV-vis spectra of anatase TiO_2 NPs, NWs and NWAs suspensions at room temperature. All the samples show relatively weak absorption in the visible region and near-infrared region. They also exhibit obvious characteristic absorption peaks in the UV region with peaks at 341 nm, 312.5 nm and 326.5 nm, respectively.

To understand the dependence of the nonlinear optical response on excitation intensity I_0, we adjusted the linear optical transmittance of the samples to the same value, approximately 77% (the corresponding concentration is 3.3×10^{-4} g/ml), and carried out

open-aperture (OA) Z-scan experiments with the laser at 532 nm, 2 kHz and 35 fs. Here I_0 is denoted as the incident intensity at the focal point. Scatter diagrams in Figs. 2(a)–2(c) are results of OA Z-scan for NP, NW and NWA suspensions at different excitation intensities. The Z-scan experiment of the pure solvent was also measured, and the results did not show any nonlinear absorption, which indicates that the contribution of the solvent can be negligible.[28]

With the variation of intensity, gradual changing processes of NLO absorption were observed. As depicted in Fig. 2(a), anatase NP suspension shows saturable absorption at low intensity of 44.4 GW/cm^2. At 113.8 GW/cm^2, it manifests a weaker signal of the valley-peak-valley type. For higher excitation intensity of 175.2 GW/cm^2, the figure of the valley-peak-valley signal becomes much more obvious. It indicates that, with increasing the excitation intensity, the contribution of two-photon absorption is enhanced and that of saturable absorption becomes weakened. The changing process suggests that two mechanisms exist simultaneously.

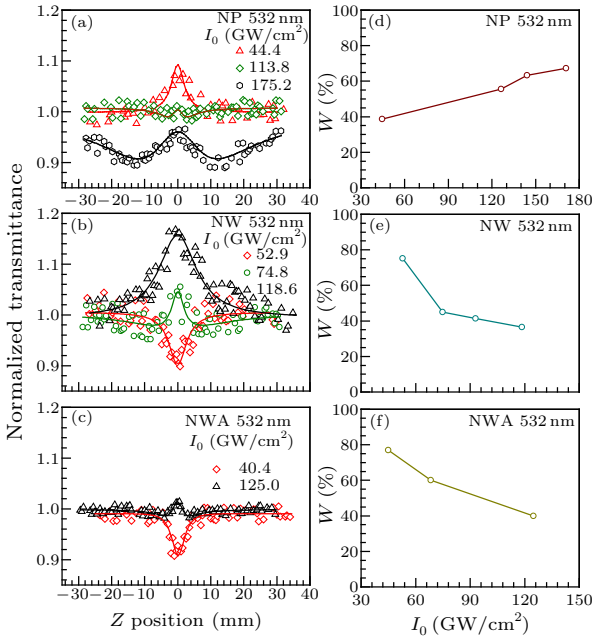

Fig. 2. OA Z-scan curves of (a) NPs, (b) NWs and (c) NWAs measured with different excitation intensities at 532 nm. (d)–(f) The trends of W as a function of the incident intensity for anatse NP, NW, NWA suspensions, respectively. W is defined as the weight of the positive absorption in experiments.

Suspensions of anatase NWs and NWAs show a similar phenomenon, but have opposite trends. As shown in Figs. 2(b) and 2(c), they all manifest reverse-saturable absorption (positive nonlinear absorption) at low intensity of 52.9 GW/cm^2 and 40.4 GW/cm^2, respectively. With the increase of intensity (74.8 GW/cm^2 and 125.0 GW/cm^2), they show a valley-peak-valley signal. This suggests the appearance of negative nonlinear absorption induced by saturable absorption. When the excitation intensity was further increased, an obvious absolute saturable absorption of NW suspensions was even observed at 118.6 GW/cm^2. The transition of anatase nanowire suspension excited by femtosecond pulsed laser in this study is similar to the phenomenon of TiO_2 nanowires' film excited by picosecond laser which was observed by Zhang *et al.*[25]

To quantitatively analyze the competitive mechanism between negative nonlinear absorption and positive nonlinear absorption in the NLO response of anatase materials, we fitted the Z-scan experimental data at a wavelength of 532 nm with the expression[25,27]

$$T(z) = W \sum_{m=0}^{\infty} \frac{q_1^m}{(1+z^2/z_0^2)^m (m+1)^{3/2}} + (1-W) \sum_{n=0}^{\infty} \frac{q_2^n}{(1+z^2/z_0^2)^n (n+1)^{3/2}}, \quad (1)$$

where $q_1 = \beta_+ I_0 L_{\text{eff}}$, $q_2 = \beta_- I_0 L_{\text{eff}}$, and β is a nonlinear absorption coefficient. The effective thickness of sample $L_{\text{eff}} = (1 - e^{-\alpha L})/\alpha$ with L being the practical thickness of the sample, 1 mm, and α being a linear absorption coefficient. Here $q_1 > 0$ and $q_2 < 0$. The first part in Eq. (1) represents the positive nonlinear absorption, the second part is the negative nonlinear absorption, and W represents the weight of positive nonlinear absorption in the total nonlinear response. The solid lines in Figs. 2(a)–2(c) are the fitting results. By fitting the experimental data of OA Z-scan, we can extract the value of W at different excitation intensities. Trends of W as a function of I_0 are shown in Figs. 2(d)–2(f). As I_0 increases, corresponding to the aforementioned analysis of competitive transformation between reverse-saturable absorption and saturable absorption, the weight of reverse-saturable absorption of NP suspensions is increased gradually, whereas the weights of saturable absorption of NW and NWA suspensions are increased. They correspond to different sensitivities of linear absorption of anatase NPs and NWs, NWAs at wavelengths near 532 nm. We contribute the differences among NPs and NWs, NWAs to their different energy structures induced by their morphologies. This also means that NLO properties of the same materials can be modulated by their morphologies.

We also used the femtosecond pulsed laser at a wavelength of 780 nm to excite the suspensions with linear transmittance of around 0.82. The corresponding concentrations of anatase NP, NW and NWA suspensions are approximately 2.5×10^{-4} g/ml. The obtained OA Z-scan results are depicted in Figs. 3(a)–3(c). As is expected, optical limiting induced by positive nonlinear absorption dominates the NLO response, which means that saturable absorption is suppressed in 780 nm. From the results we can see that the nonlinear absorptions of NWs and NWAs in Figs. 3(b) and 3(c) are more sensitive to excitation intensity than NPs in Fig. 3(a). The sensitivity of absorption to excitation intensity is related to the bulk region effect, and the larger the bulk region is,

the more sensitive the absorption is to the excitation intensity.[29] It is worth noticing that the length of nanowires is approximately 70–400 nm, which is longer by a factor of 4–25 than diameters of NPs with size of 16 nm. Thus we attribute the sensitivities of NWs and NWAs to its larger bulk region, which means that NWs and NWAs would possess the stronger bulk properties. We also contribute the nonuniformity of NWs and NWAs with different lengths of 70–400 nm to another reason of the sensitiveness.[30]

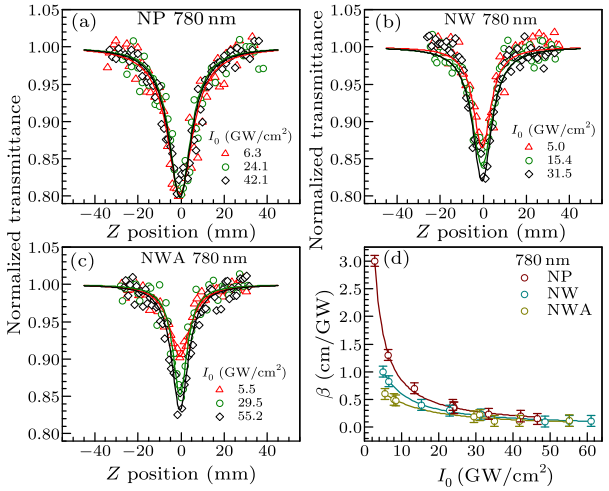

Fig. 3. OA Z-scan curves of (a) NPs, (b) NWs and (c) NWAs with different incident intensities at 780 nm. (d) The effective nonlinear optical absorption coefficients β as a function of the incident intensity.

To quantitatively analyse the nonlinear optical response, the Z-scan theoretical formula is used to fit OA Z-scan data as the solid lines in Figs. 4(a)–4(c),[25,27]

$$T_{\mathrm{OA}}(z) = \sum_{m=0}^{\infty} \frac{(-\beta I_0 L_{\mathrm{eff}})^m}{(1+z^2/z_0^2)^m (m+1)^{3/2}}. \qquad (2)$$

Nonlinear absorption coefficients of the samples β are obtained and their values are plotted as a function of I_0, as shown in Fig. 3(d). At low intensity, β of NP suspensions is the largest of three samples. The results also satisfy the above judgment that NWs and NWAs possess a stronger bulk region effect. In other words, NPs with smaller size possess a larger quantum confinement region. Normally, the larger the quantum confinement region is, the greater the nonlinear optical properties are.[31,32] It is reported that the bulk TiO_2 has a weaker nonlinearity optical property than nanostructured TiO_2.[22,33] Thus nonlinearity of NPs is supposed to be larger than NWs and NWAs. Another reason may be that NPs possess the larger absorption cross section, which is induced by surface defect states, oxygen vacancies and higher surface-volume ratio.[15,23,34] At low intensity, β of NWAs is smaller than NWs. We contribute it to the effect of the well-defined structure of NWAs, which possess lower lattice defects, surface defects and residual stress after annealing.[35,37] It could be noticed that, with the increase of the incident intensity, β of all the three samples gradually tends to be equal. As the incident intensity becomes higher, β becomes smaller. It is demonstrated that effects of morphologies and defects only work at low intensity. With increasing the intensity, the same materials' NLO absorption coefficients β become closer to the same value, though they have different morphologies and surface structures. At high intensity, nonlinear optical absorption coefficients of the three samples all did not have any more changes, which agrees with the phenomenon of pure third-order nonlinearities of PMMA-TiO_2 film (T60) observed at 780 nm.[22] Thus morphologies, defects and excitation intensity all play important roles in NLO response, whereas effects of the morphologies and defects are conditioned by excitation intensity and only manifest at low intensity. As $\alpha = \alpha_0 + \beta(I)I$, $\beta(I) = \alpha_2 + \alpha(I)$,[31] α, α_0, $\beta(I)$ are the total absorption coefficient, linear absorption coefficient and nonlinear absorption coefficient, respectively, α_2 and $\alpha(I)$ are third-order and higher-order nonlinear absorption coefficients. The trends of β as a function of I_0 in Fig. 3(d) show that higher-order nonlinear absorption occurs in the processes. It is explained that the different sensitivities of 532 nm and 780 nm to excitation intensity are a reflection of the fact that a laser energy of 532 nm (2.33 eV) is closer to the band gap of anatase TiO_2 (~3.2 eV). With excitation energy closer to the band gap of the material, the nonlinear optical response becomes more sensitive to excitation intensity I_0.

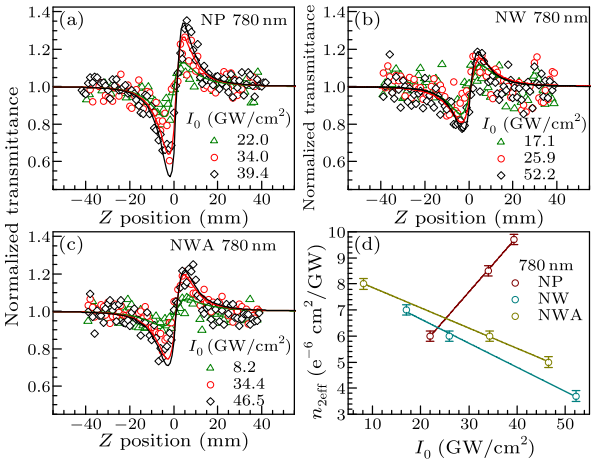

Fig. 4. CA Z-scan results of (a) NPs, (b) NW and (c) NWA suspensions measured with different intensities at 780 nm.(d) Variation of the effective nonlinear refraction index $n_{2\mathrm{eff}}$ as a function of the incident intensity.

Scatter diagrams in Figs. 4(a)–4(c) are closed-aperture (CA) Z-scan results of NP, NW and NWA suspensions divided by OA Z-scan results at a wavelength of 780 nm. The solid lines are fitting results by the following CA Z-scan theoretical formula[15,24,27]

$$T_{\mathrm{CA}}(z)/T_{\mathrm{OA}}(z) = 1 + \frac{4\Delta\varphi_0 z/z_0}{((z/z_0)^2+9)((z/z_0)^2+1)}. \qquad (3)$$

Change of wavefront phase at focus $\Delta\phi_0$ =

$2\pi n_{2\text{eff}} I_0 L_{\text{eff}}/\lambda$ with $n_{2\text{eff}}$ being a nonlinear refractive index. All the samples show a valley-peak configuration, a symbol of self-focusing phenomenon ($n_{2\text{eff}} > 0$). As shown in Fig. 4(d), all the nonlinear refractive index $n_{2\text{eff}}$ of the three samples behave in a linear relationship with I_0. Here $n_{2\text{eff}}$ of NPs is correlated with I_0 positively. On the contrary, n_2 of NW and NWA shows negative correlation with I_0. Linear trends in Fig. 4(d) suggest that a higher-order nonlinear refractive process happens, which is corresponding to the trends of nonlinear absorption coefficients in Fig. 3(d).[31,37]

Table 1. The NLO constants of samples and the references, with λ being the wavelength. Here $n_{2\text{eff}}$ is in units of $10^{-18}\,\text{m}^2/\text{W}$.

λ (nm)	Sample	β (10^{-11} m/W)	$n_{2\text{eff}}$	
532	NP	6.46 (& −4.24)		Present
	NW	3.48 (& −3.60)		
	NWA	3.83 (& −2.54)		
780	NP	3–0.15	0.6–0.97	Present
	NW	1–0.11	0.7–0.37	
	NWA	0.6–0.12	0.8–0.5	
532	NP	22.06	34.77	Ref. [15]
	NW	16.85	17.38	

In Table 1, we list the results of NLO parameters of 532 nm and 780 nm with other reported results. The examined values of β at 532 nm and 780 nm are all smaller by 1–2 orders of magnitude than the results of Ref. [15], which were tested with a nanosecond laser. Small values of β and n_2 are supposed to have a relationship with the excitation laser source. As we all know, compared with the nanosecond and picosecond laser with longer pulse duration, the femtosecond laser with ultrashort pulse in our experiments can effectively reduce the thermal effect, electric scaling and nonlinear polarization, which all need a longer response time.[38] We should also notice that transmittance of our suspensions can reach up to 77% or 82%, which are higher than the value of 70% in Ref. [15]. This means that the content of anatase is very small. Anatase suspensions with low concentration are just as the nanoporous film with high porosity. Here n_2 of the nanoporous film ($1 \times 10^{-19}\,\text{m}^2/\text{W}$) is smaller by a factor of 25 than the values of pure rutile TiO_2, which were expected to be due to the reduced density of TiO_2 (35%).[3] Therefore, the estimated small values of β and n_2 for anatase suspensions at 532 nm and 780 nm are relevant to the low concentration. For the NLO parameters at 780 nm, they are smaller than results of 532 nm. This may be due to the fact that energy of laser at 780 nm is further away from anatase's band gap than that of 532 nm.

In summary, nonlinear optical properties of anatase NP, NW and NWA suspensions have been investigated using the Z-scan technique at 532 nm and 780 nm. At 532 nm, the OA Z-scan results of anatase NPs and NWs, NWAs show opposite competitive transitions between positive absorption and negative absorption. When examined at 780 nm, all the samples only show reverse-saturable absorption at different intensities. NLO absorption coefficients at 780 nm are compared and follow the order NPs≥NWs≥NWAs. It is assumed that the morphology of NPs with higher surface-to-volume ratio and defects of NWs strengthen the NLO phenomenon. The present results also show that effects of shape and defects on NLO response are conditioned by excitation intensity and only manifested at low intensity. Nonlinear refractive indexes of all the samples show a linear relationship with excitation intensity at 780 nm. As the laser at 532 nm is closer to the band gap of anatase TiO_2, NLO absorption of anatase at 532 nm shows greater sensitivity to excitation intensity than that of 780 nm. This study would provide further guidance for applications of nanostructured anatase in solar cells, optoelectronic devices or other aspects.

We thank Zhaoyang Fan in the Department of Chemistry and Biochemistry, Texas Tech University, Lubbock, Texas for providing anatase TiO_2 powders.

References

[1] Fujishima A and Honda K 1972 *Nature* **238** 37
[2] Li C et al 2016 *Acta Phys. Sin.* **65** 037102 (in Chinese)
[3] Portuondo-Campa E et al 2008 *J. Chem. Phys.* **128** 244718
[4] Wang G M, Wang H Y, Ling Y C, Tang Y C, Yang X Y, Fitzmorris R C, Wang C C, Zhang J Z, Li Y et al 2011 *Nano Lett.* **11** 3026
[5] Li S P et al 2015 *RSC Adv.* **5** 1902
[6] Kuralay F et al 2016 *Talanta* **160** 325
[7] Albelda J A V et al 2017 *Biosensors Bioelectronics* **89** 518
[8] Hazra A et al 2013 *Sens. Actuators B: Chem.* **183** 87
[9] Ma H C et al 2015 *Electrochem. Commun.* **57** 18
[10] Xiong J et al 2014 *Org. Electron.* **15** 835
[11] Xiong J et al 2014 *Org. Electron.* **15** 1745
[12] Wang X X et al 2015 *Curr. Appl. Phys.* **15** 662
[13] Sugimoto T, Zhou X P and Muramatsu A 2003 *J. Colloid Interface Sci.* **259** 43
[14] Chen D H and Caruso R A 2013 *Adv. Funct. Mater.* **23** 1356
[15] Divya S et al 2014 *Appl. Phys.* A **114** 1079
[16] Yang Z et al 2015 *Acta Phys. Sin.* **64** 177901 (in Chinese)
[17] Zhao M et al 2016 *Chin. Phys. Lett.* **33** 104201
[18] Wang Y W, Liu S, Zeng B W, Huang H, Xiao J, Li J B, Long M Q, Xiao S, Yu X F, Gao Y L, He J et al 2017 *Nanoscale* **9** 4683
[19] Xiao S et al 2015 *Opt. Express* **23** 5875
[20] Zhang J D et al 2016 *Opt. Lett.* **41** 1704
[21] Wang Y Q et al 2014 *Acta Phys. Sin.* **63** 144204 (in Chinese)
[22] Elim H I et al 2003 *Appl. Phys. Lett.* **82** 2691
[23] Gayvoronsky V et al 2005 *Appl. Phys.* B **80** 97
[24] Divya S et al 2014 *Chin. Phys.* B **23** 084203
[25] Zhang K et al 2011 *Opt. Lett.* **36** 3443
[26] Pan X et al 2012 *ACS Appl. Mater. Interfaces* **4** 3944
[27] Sheik-Bahae M et al 1990 *IEEE J. Quantum Electron.* **26** 760
[28] Wang Y Q et al 2015 *Acta Phys. Sin.* **64** 034214 (in Chinese)
[29] Xu J L et al 2015 *Sci. Rep.* **5** 14856
[30] Wang Y W et al 2016 *Sci. Rep.* **6** 33070
[31] He J et al 2004 *J. Appl. Phys.* **95** 6381
[32] Neo M S et al 2009 *J. Phys. Chem.* C **113** 19055
[33] Watanabe Y, Ohnishi M and Tsuchiya T 1995 *Appl. Phys. Lett.* **66** 3431
[34] Xiong J et al 2016 *Org. Electron.* **30** 30
[35] Yan T F et al 2015 *Chin. Phys. Lett.* **32** 077801
[36] Tong X H, Zhang H and Li D Y 2015 *Sci. Rep.* **5** 8459
[37] Gu B, Sun Y and Ji W 2008 *Opt. Express* **16** 17745
[38] Wang Y W et al 2015 *Appl. Phys. Lett.* **107** 091905